Transactions of the Korean Nuclear Society Autumn Meeting
Goyang, Korea, October 24-25, 2019

Optimization of a Plastic Scintillator for Neutron Detection

Wooseub Kim [a], Minhwan Kim [a], Kilyoung Ko [a], and Gyuseong Cho [a*]
[a]*Department of Nuclear and Quantum Engineering, Korea Advanced Institute of Science and Technology,*
291 Daehak-ro, Yuseong-gu 34141, Daejeon, Republic of Korea
[*]*Corresponding author: gscho@kaist.ac.kr*

1. Introduction

X-ray imaging applications have been widely used for nondestructive testing to evaluate the integrity and properties of material or components without causing damage to the tested object. However, the x-ray has a disadvantage that they rarely penetrate the materials with high atomic numbers. Unlike the behavior of the x-ray, neutron has a high penetrating power for metals, but a low penetrating power for hydrogen compounds because the neutron reacts only with atomic nucleus. In this aspect, neutron radiography can be complementary to the X-ray imaging applications. To prepare the neutron radiography system using indirect-conversion detectors, the selection of an appropriate scintillator is a key part to effectively absorb the neutron energy emitted from a neutron source, and consequently to achieve enough signals for high quality neutron images.

In this study, as a promising candidate for neutron detection, a plastic scintillator (Eljen, EJ-200) was examined and optimized to maximize the number of optical photons reaching a photodetector. To identify variations in the neutron energy absorbed by the plastic scintillators with different thicknesses, Monte Carlo N-Particle Transport Code 6 (MCNP 6) was used for radiation transport simulation. Based on the MCNP 6 simulation results, optical design software LightTools was additionally used to compare and enhance the light collection efficiency of the plastic scintillator by assuming that various reflector materials were covered on the surface of the plastic scintillator, respectively. The results show that the 5 cm thick plastic scintillator covered with a Teflon film is superior to the other cases when our electronic neutron generator is used for neutron radiography.

2. Methods and Results

2.1 Description of scintillator

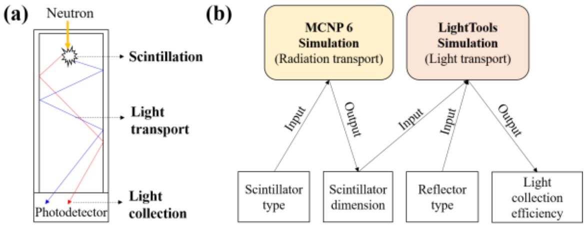

Fig. 1. (a) General description of scintillation process, and (b) schematic workflow for scintillator optimization.

As shown in Fig. 1(a), the scintillation process is one of luminescence whereby light of a characteristic spectrum is emitted following the absorption of radiation. When neutrons deposit their energy at the volume of a scintillator, the energy is partially converted to optical photons. Then, the optical photons transmitted from the scintillator encounter a photodetector and contribute to electrical signals. For those reasons, the light collection efficiency of a scintillator, as well as the number of optical photons emitted from the scintillator, has a decisive effect on the quality of neutron images. Thus, the simulations of radiation and light transport were conducted to optimize the plastic scintillator.

In this study, the active area of a photodetector was assumed to be a size of 10 × 10 mm. To ideally attach the plastic scintillator to the photodetector, the plastic scintillator should have the same area and base shape as the photodetector. Therefore, only by varying the scintillator thickness, the total neutron energy absorbed by the plastic scintillator was examined through the MCNP 6 simulation. The light collection efficiency of the scintillator covered with a reflector material was derived by LightTools simulation. The scintillation efficiency of the plastic scintillator was considered as 10,000 photons/MeV [1]. Based on the simulation results depending on scintillator thickness and reflector materials, the number of optical photons reaching the photodetector under neutron irradiation (N) was calculated using equation (1).

$$N = E \times I \times \eta \,, \qquad (1)$$

where E is the total neutron energy absorbed by a scintillator in MeV, I is the scintillation efficiency of a scintillator in photons/MeV, and η is the light collection efficiency of a scintillator. By comparing the value of N in each scenario, we found the optimal scintillator thickness and the proper reflector material.

2.2 Radiation transport simulation

The neutron energy spectrum from our electronic neutron generator is shown in Fig. 2. The neutron energy spectrum and the material composition data for the plastic scintillator and surroundings were applied to the MCNP 6 simulation [1, 2]. To conservatively evaluate the impact of scattered neutrons on the plastic scintillator array, the three plastic scintillators were positioned in a row as shown in Fig. 3. The centrally located plastic scintillator was defined as “center”.

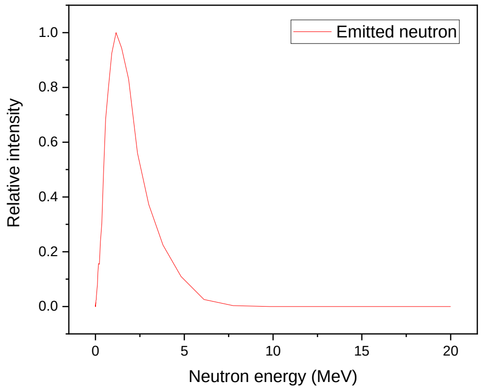

Fig. 2. Neutron energy spectrum from our electronic neutron generator.

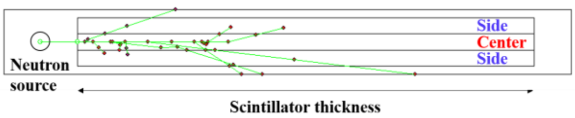

Fig. 3. Simulated geometry using MCNP 6.

The neutron source was set to a pencil beam and located 1 cm away from the centrally located plastic scintillator. Total absorbed neutron energy, and neutron energy absorbed per unit volume of the three plastic scintillators were derived by the MCNP 6 simulation, respectively. To identify the noise effects from naturally-occurring background radiation, the representative gamma energies of 57.7 keV and 1.7645 MeV released through the natural decay series of U-238 and Th-232 were additionally applied to the MCNP 6 simulation.

2.3 Light transport simulation

In general, aluminum, Enhanced Specular Reflector (ESR) film, and Teflon (PTFE) film are popularly used for light reflectors. The Teflon film has the characteristics of Lambertian reflectance while the reflectance distribution of the aluminum and the ESR film is specular as shown in Fig. 4. Because the value of the reflectance for the ESR film in the wavelength of 425 nm, which is the maximum emission wavelength of the plastic scintillator, is higher than that for the aluminum, the ESR film was simulated instead [1].

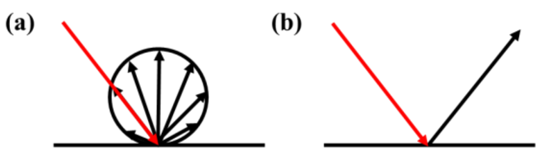

Fig. 4. Characteristics of (a) Lambertian reflectance, and (b) specular reflectance.

Table I: Optical properties in the wavelength of 425 nm.

Optical properties (Unit)	Component (Material)	Value
Refractive index (None)	Scintillator (PVT)	1.58
Attenuation length (cm)	Scintillator (PVT)	380
Reflectance (%)	Reflector (ESR)	98
	Reflector (PTFE)	98

The optical properties of the plastic scintillator and the selected reflector materials are summarized in Table I [1, 3, 4]. The number of optical photons emitted from a scintillator is proportional to the amount of radiation energy absorbed by the scintillator. Thus, the MCNP 6 simulation results for the neutron energy absorbed per unit volume of the plastic scintillator were used and converted to weighting factors in order to differentially generate optical photons at the plastic scintillator.

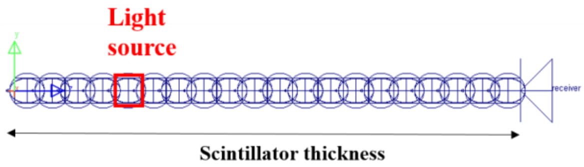

Fig. 5. Simulated geometry using LightTools.

For light transport, simulated geometry using Light Tools is shown in Fig. 5. The entire volume of the plastic scintillator was divided into the 1 cm^3 volumes, respectively. Then, the number of optical photons was differentially generated inside of the separated volumes. To identify the light collection efficiency of the plastic scintillator, the number of optical photons reaching the "receiver" where the photodetector will be located was counted.

3. Results and discussion

Figs. 6 and 7 presented by the MCNP 6 simulation results show that as the plastic scintillator thickness increases, the amount of neutron energy absorbed by the plastic scintillator tends to increase. However, the difference in the total absorbed neutron energy get reduced. The effect of scattered neutrons, which would be an image noise, was not considerable.

Fig. 8 shows that the difference of the total absorbed neutron energy between the 10 cm and 20 cm thick plastic scintillators was not significant compared to the 5 cm thick plastic scintillator. This result was derived without the use of Gaussian energy broadening function because actual neutron spectra measured by the photodetector were not able to be obtained. Furthermore, only the neutron energy range from 0.2 MeV to 1 MeV was selectively presented to clearly compare the intensity difference depending on the scintillator thickness. Table II summarizes the total neutron energy absorbed by the plastic scintillators with various thicknesses.

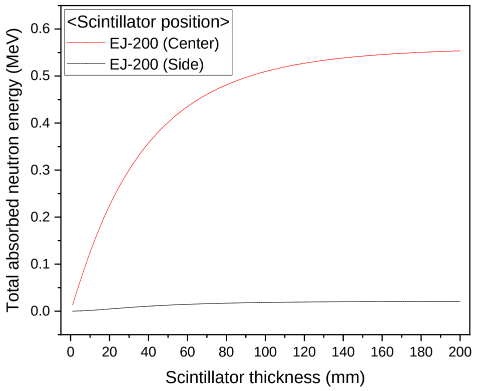

Fig. 6. Total neutron energy absorbed by the plastic scintillator as a function of scintillator thickness.

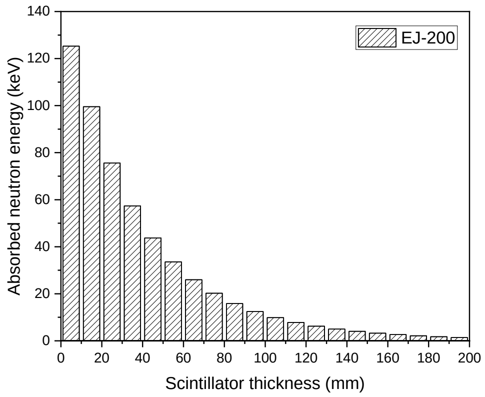

Fig. 7. Neutron energy absorbed per unit volume of the plastic scintillator as a function of scintillator thickness.

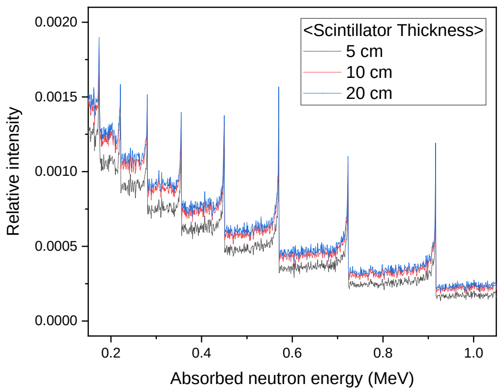

Fig. 8. Variations in neutron intensity reacted to the plastic scintillators with the thicknesses of 5 cm, 10 cm, and 20 cm.

Table II. Total neutron energy absorbed by the plastic scintillators with the thicknesses of 5 cm, 10 cm, and 20 cm.

Scintillator thickness	Total absorbed neutron energy (MeV)
5 cm	0.40
10 cm	0.51
20 cm	0.55

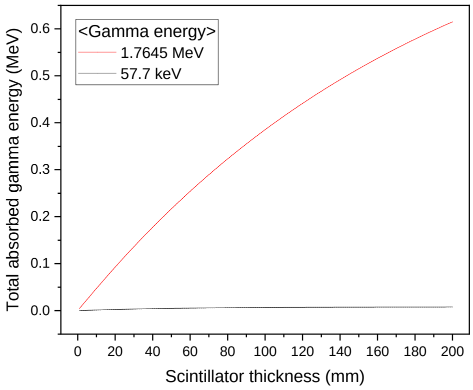

Fig. 9. Total gamma energy absorbed by the plastic scintillator as a function of scintillator thickness.

Fig. 9 shows that the amount of gamma energy absorbed by the plastic scintillator increases with increasing scintillator thickness. Especially, the 1.7645 MeV gamma ray is greatly affected by the scintillator thickness compared to the 57.7 keV gamma ray.

Table III. Light collection efficiency of the plastic scintillators with the thicknesses of 5 cm, 10 cm, and 20 cm depending on reflector materials.

Scintillator thickness	Light collection efficiency (%)	
	ESR film	Teflon film
5 cm	41	56
10 cm	37	18
20 cm	24	2

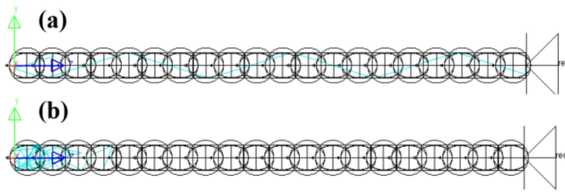

Fig. 10. Behavior of light inside the plastic scintillators covered with (a) the ESR film, and (b) the Teflon film.

As shown in Table III, the light collection efficiency decreases with increasing scintillator thickness. Since most neutrons deposit their energy at the front of the plastic scintillator, optical photons are mostly emitted from the front of the plastic scintillator and it is more difficult for such optical photons to reach the receiver when the scintillator thickness becomes longer. The

Teflon film is found to be an outstanding reflector for the 5 cm thick plastic scintillator, but the ESR film is more suitable for the 10 cm and 20 cm thick plastic scintillators. Fig. 10 shows the behavior of light inside the plastic scintillator depending on reflector materials.

Table IV. The number of optical photons reaching the photodetector under neutron irradiation.

Scintillator thickness	**The number of optical photons reaching the photodetector**	
	ESR film	Teflon film
5 cm	1700	2200
10 cm	1900	900
20 cm	1300	100

From the MCNP 6 and LightTools simulation results, the number of optical photons reaching the photodetector under neutron irradiation was calculated, as shown in Table IV, by considering the total neutron energy absorbed by the plastic scintillator and the light collection efficiency of the plastic scintillator simultaneously. It was verified that the 5 cm thick plastic scintillator covered with the Teflon film is superior to the other cases. Moreover, the 5 cm thick plastic scintillator is less sensitive to background radiation than the 10 cm and 20 cm thick plastic scintillators as proven in Fig. 9.

4. Conclusion

In this research, the EJ-200 plastic scintillator was selected as a promising candidate for neutron detection. Based on the neutron energy spectrum from our electronic neutron generator and the material composition data for the plastic scintillator, the MCNP 6 simulation was conducted to identify variations in absorbed neutron energy, the impact of scattered neutrons, and the noise effects from background radiation. The results presented by the MCNP 6 simulation, as well as the optical properties of the plastic scintillator and several reflector materials, were applied to the LightTools simulation in order to figure out the light collection efficiency of the plastic scintillator. When it comes to the number of optical photons reaching the photodetector under neutron irradiation and the noise minimization from background radiation, the results confirmed that the 5 cm thick plastic scintillator covered with the Teflon film is superior to the other cases.

5. Acknowledgements

This work was supported by the Nuclear Research & Development Program of the National Research Foundation of Korea (NRF) grant funded by the Ministry of Science, ICT and Future Planning (MISP) (Grant code: 2017M2A2A6A02020807, 2018M2A8A5023361).

This work was partly supported by a National Research Foundation of Korea (NRF) grant funded by the Korean government (MSIP) (NRF-2017M2A8A50 15084).

REFERENCES

[1] Eljen Technology, General Purpose Plastic Scintillator EJ-200, EJ-204, EJ-208, EJ-212, Available from: https://eljentechnology.com/images/products/data_sheets/EJ-200_EJ-204_EJ-208_EJ-212.pdf.

[2] R. J. Mc Conn, C. J. Gesh, R. T. Pagh, R. A. Rucker, and R. G. Williams, Compendium of Material Composition Data for Radiation Transport Modeling, Revision 1, Pacific Northwest National Laboratory, U.S. Department of Energy, 2011.

[3] 3M Optical Systems, Vikuiti^{TM} Enhanced Specular Reflector (ESR), Available from: http://multimedia.3m.com/mws/media/721799O/vikuititm-enhanced-specular-reflector-esr.pdf.

[4] Berghof, Optical PTFE The reference for light, Available from: https://www.berghof-fluoroplastics.com/fileadmin/Dateien-Einpflege/Seitenbaum/Home-Downloads/Produkte/PTFE-Produkte/Optisches%20PTFE/Berghof_PTFE-Products_Optical-PTFE.pdf.